AIAA JOURNAL
Vol. 47, No. 5, May 2009

Open-Loop Control of Disk Wakes

Rory P. Bigger,* Hiroshi Higuchi,† and Joseph W. Hall‡
Syracuse University, Syracuse, New York 13244

DOI: 10.2514/1.39108

Open-loop control in the near wake of a disk in subsonic air and water flows was investigated using particle image velocimetry at a Reynolds number based on the disk diameters of 67,000 and 20,000, respectively. The air model had tabs along the edge that were driven radially by electromagnetic actuators, and the water model had slots connected to a piston and cylinder external to the flow. In both systems, the frequency of actuation could be varied, and in air, the spatial extent of the forcing could be controlled. Symmetrical actuation produced a reduction in the recirculation-region length of 10% for both air and water. Additionally, a helical excitation at the fundamental natural vortex-shedding frequency in air caused a reduction of 15% and caused the wake to oscillate strongly in phase with the excitation. The most effective symmetrical actuation frequencies correspond to twice the natural frequency of the asymmetric mode in the unforced wake. The effects of actuation on the instantaneous and mean velocity fields are presented and discussed in detail.

Nomenclature

C_{p_b}	=	base pressure coefficient: $(p_b - p_\infty)/q_\infty$
$C_{p_b(\mathrm{NA})}$	=	base pressure coefficient without actuation
C_μ	=	momentum coefficient, $4h_{\mathrm{jet}}u_{\mathrm{jet,MS}}/(DU_\infty^2)$
D	=	diameter of disk
f	=	frequency
h_{jet}	=	slot thickness on water disk model
p_b	=	base pressure
q_∞	=	freestream dynamic pressure
Re_D	=	Reynolds number based on diameter, $U_\infty D/\nu$
r	=	direction normal to the flow (radial direction)
St	=	Strouhal number (nondimensional frequency), fD/U_∞
St_e	=	excitation (actuation) Strouhal number
U_∞	=	freestream velocity
u	=	velocity component in the x direction
u_{jet}	=	velocity at the jet exit on the water model normal to the jet
u'	=	velocity fluctuation in the x direction
v	=	velocity component in the r direction
v'	=	velocity fluctuation in the r direction
x	=	direction of the flow (streamwise direction)
ν	=	kinematic viscosity

I. Introduction

PREVIOUS attempts at controlling the wake behind axisymmetric bluff bodies have traditionally focused on altering the boundary-layer development to shift the separation point. This may be accomplished by passive means, for example, as occurs on the seams on sporting balls [1]. In particular, Kiura and Higuchi [2] and Higuchi [3] showed that the seams on a baseball modify the boundary-layer separation and are responsible for the side-force variation in knuckleballs. To control the flow over a sphere, Jeon et al. [4] used periodic blowing and suction through a slit; this caused flow separation to be delayed, resulting in a smaller wake region and reduced drag. Another means of passive control are grooves along the body in the streamwise direction, such as those used by Quass et al. [5] to reduce drag. In addition to passive control, active control techniques may also be used. Amitay et al. [6], for example, used a synthetic jet mounted on a circular cylinder to modify the pressure gradient along the cylinder surface, thereby controlling separation. Cannon [7] and Higuchi et al. [8] were able to perform passive control of a disk wake by adding porosity and causing effects similar to using base bleed (see [9,10]). The wake behind a solid disk poses a great control challenge, as the separation point is fixed and thus cannot be affected by the previously mentioned boundary-layer manipulations. To make flow control on the disk even more challenging, the wake becomes fully turbulent for Reynolds numbers as low as 2000 [11] and is quite three-dimensional [12]. Despite these difficulties, Berger et al. [13] were able to enhance a helical mode in the disk wake through active control by oscillating the disk itself in a nutation mode.

Because passive control and basic active control have been previously demonstrated to have some success in controlling the disk wake and because there is no means of forcing a boundary layer on the disk, the goal of the present study was to determine if the separated shear layer itself could be controlled. This investigation consisted of two complementary studies in air and in water. In air, a model was built that contained movable tabs on the edge controlled by electromagnet actuators. In water, electromagnets could not be used and, instead, a system employing an externally mounted piston and cylinder system pumping through slots in the disk was used. This system was first developed for flow control on an airfoil (see [14]). The frequency of actuation for this system was set manually and checked with a laser Doppler velocimetry (LDV) system. In both air and water, the effects of periodic forcing at the disk edge were investigated using particle image velocimetry (PIV) measurements. In air, a high-resolution PIV system was used, whereas the slower flow speed of water was better suited to the use of a time-resolved system (TR-PIV), allowing the complementary study to use the benefits of both systems.

II. Experimental Setup

The experiments were performed in the subsonic wind-tunnel and large water-channel facilities at Syracuse University. Both tunnels have a test section of $0.61 \times 0.61 \times 2.44$ m ($2 \times 2 \times 8$ ft). The results presented correspond to $Re_D = 67,000$ for air and 20,000 for water. In both cases, the disk model was mounted on a streamlined

Presented as Paper 3187 at the 3rd AIAA Flow Control Conference, San Francisco, CA, 5–8 June 2006; received 13 June 2008; revision received 30 January 2009; accepted for publication 3 February 2009.

*Currently Graduate Student, Department of Mechanical Engineering, Pennsylvania State University, University Park, PA 16802; bigger@psu.edu. Member AIAA.

†Professor and Program Director, Department of Aerospace Engineering, 141 Link Hall; hhiguchi@syr.edu. Associate Fellow AIAA.

‡Currently Assistant Professor, University of New Brunswick, Fredericton, NB, E3B 5A3, Canada; jwhall@unb.ca. Member AIAA.

strut via a sting. In air, this allowed a path through which the electrical cables to the actuators could be passed, and in the water channel, this provided a path for water to be injected for control. PIV systems were used to measure the velocity field in both air and water. Additionally, an LDV system was used in water to calibrate the actuators. The coordinate system used has its origin in the center of the trailing edge of the disk, where x is the freestream direction and r is the radial direction. All coordinates were normalized by the disk diameter.

A. Wind-Tunnel Model

The model used in air had a leading-edge diameter of 0.102 m, with a beveled edge tapered to 0.092 m at the trailing edge. The overall thickness was 0.015 m, and 6 TDK P1002A electromagnet actuators were installed inside the disk. These actuators moved 6 equally spaced segments of the disk edge covering half of the circumference in the radial direction. A sketch of the disk and a photograph of the actuators are shown in Fig. 1. The disk was also equipped with a transducer for measuring the base pressure. When the actuators were in the retracted position, the edge segments lay flush with the disk edge, and the actuators could move outward up to 2 mm in the radial direction. An analog signal from a National Instruments D/A processor was sent to each actuator through individual Kemo M32 audio power amplifiers. The time-dependent displacement was checked with a laser displacement meter, and frequency was also monitored with a strobe light.

B. Water-Channel Model

The disk used in water had a diameter of 0.102 m, the same as in air, and a thickness of 0.013 m. Photographs of the disk model and the piston system are shown in Fig. 2. The disk was constructed from polyvinyl chloride with channels milled inside to connect to a single stainless steel inlet pipe. From the inlet, the path was split into 6 channels ending in thin (0.00239 m) slots covering half of the circumference, the same as the tabs in air. The result is a zero-net-mass actuator system with suction and blowing occurring through the slots. To drive this suction and blowing, the inlet pipe was connected to a piston and cylinder external to the flow via a Swagelock fitting to a semiflexible nylon tube. The piston bore was 0.022 m and the stroke was 0.032 m. The cylinder and pipe were filled entirely with water to link the top of the cylinder to the slots as directly as possible, eliminating potential compression effects if air was in the system. The piston, and therefore the fluid, was driven by a $\frac{1}{3}$ hp General Electric Company ac motor powerful enough to drive water into 6 pistons with individual phase settings, though only one piston was used here. The motor contains a gearbox with a hand crank for setting its frequency. Preliminary calibration of frequency was done with a strobe light, but the velocity-time trace was measured at the slot exits with the LDV system as a final check. Additionally, using the velocity-time trace, the momentum coefficient based on the mean square jet exit velocity and the slot area normalized by the disk area was found to range from $C_\mu = 6 \times 10^{-4}$ to 4×10^{-3} for the actuation frequencies used in the experiment.

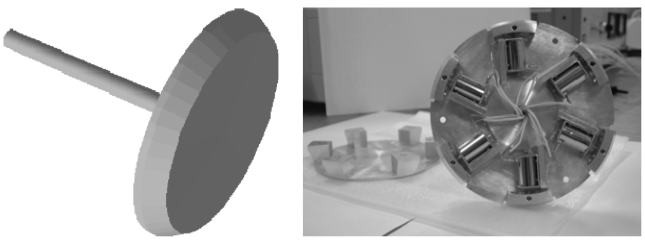

Fig. 1 Sketch of wind-tunnel disk model (left) and a photograph of the actuators inside (right).

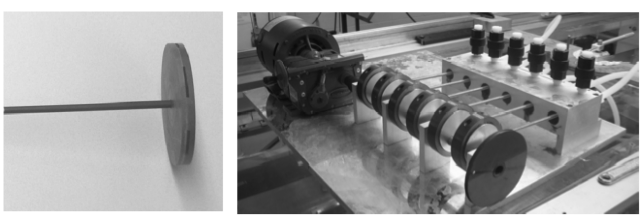

Fig. 2 Water-tunnel disk model (left) and actuator system (right).

C. Data Acquisition Equipment

Velocity-time histories were measured in air with a constant-temperature hot-wire anemometer in the initial investigation of the natural frequency of the wake. Likewise, a LDV system (TSI, Inc.) was used for the same purpose in water. In water, it was also used to check the actuation signal at the jet exits. For the remainder of the results, PIV was used. In air, a DANTEC 2-component PIV system with a 200 mJ double-cavity Nd:YAG laser was used. Olive oil seeding with a mean particle diameter of 5 μm was introduced near the downstream diffuser in the wind tunnel with a Laskin nozzle seeder. In water, a DANTEC time-resolved (TR-PIV) system was used. This unit has a maximum frame-capture rate of 4000 Hz, but with the slow flow speeds in water, only 125 Hz maximum was used. This is still much faster than the stereo PIV system used in air and allows for velocity-time traces across the entire flowfield. The water was uniformly seeded with neutrally buoyant polyamid seeding particles with a diameter of 50 μm.

D. Natural Frequency and Actuator Setup

The shear layer was forced at the natural frequency of the dominant helical structure in the wake or at harmonics of this frequency. In [13,15] this frequency was found to be to be $St = 0.135$ behind a thin disk. Balligand [15] found that the dominant mode was strong at one diameter downstream and became somewhat intermittent at positions further downstream. With this in mind, the velocity was measured at $x/D = 1$ and $r/D = 1$, a radial position outside of the shear layer for a clean signal in the water channel. In air, the velocity was sampled further downstream at $x/D = 2.5$ and $r/D = 0.45$ to capture the forming helical mode and to keep the hot-wire probe out of the reverse-flow region. Power spectra taken from the velocity-time traces at these points indicate that the largest peaks in the spectra are $St = 0.15$ in air and $St = 0.14$ in water. Both values are higher than those recorded in [13,15], and the differences can be attributed to the thicker disks used in the current study.

The frequency and phase of the actuators in air were accurately controlled using software. Because each actuator could be driven on its own, there were a number of possibilities for actuation schemes. Those used for comparison in this paper are sketched in Fig. 3 (for other modes tested, including staggered excitation, see [16]). The symmetric mode was actuated at $St_e = 0.30$, or twice the fundamental, to better force the asymmetric structure. The helical excitation was forced at $St_e = 0.15$, the natural frequency of the structure; both rotational directions were tested and produced identical results. The displacement time trace was also found to be near sinusoidal. The water-channel model could only be forced symmetrically, due to limitations of the system. Velocity-time traces were taken at different slot exits and found to be symmetric at opposite radial positions. The frequency content of the actuator output is shown in Fig. 4. The signal shows harmonics due to a slightly higher-order waveform, but most of the energy is associated with the first peak, indicating that the excitation is primarily sinusoidal. In the experiment, the wake was forced at both $St_e = 0.14$, the fundamental, and $St_e = 0.28$, the first harmonic.

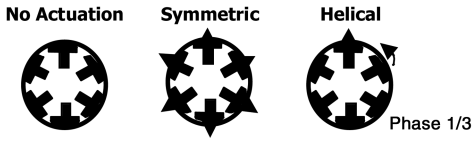

Fig. 3 Wind-tunnel model actuation modes.

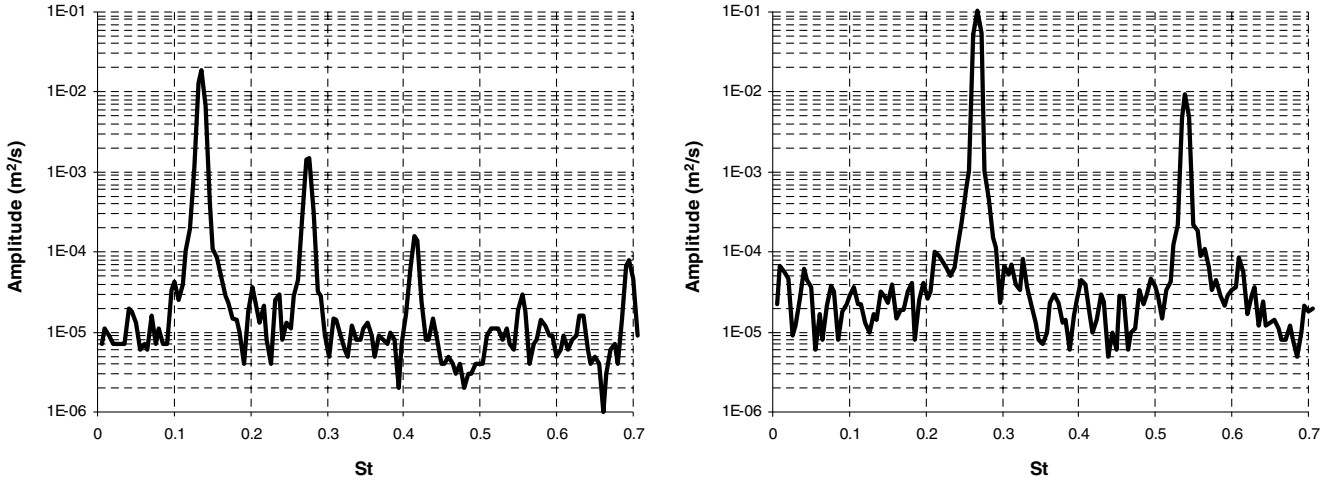

Fig. 4 Power spectra of the forcing signals in water: a) $St_e = 0.14$ symmetric actuation and b) $St_e = 0.28$ symmetric actuation.

III. Experimental Results

All velocity measurements were performed using PIV systems. In air, the 2-component PIV system allows for capturing of instantaneous snapshots of data, but the subsequent velocity field snapshots are without sufficient time resolution for any frequency analysis. The snapshots are essentially random samples that can be ensemble-averaged to observe the mean flow. To get the mean flow in water with the TR-PIV system, several short-duration time-dependent ensembles were captured. Each time average contained about 16 s of data, enough for roughly four cycles of the $St_e = 0.14$ mode. For frequency analysis, the TR-PIV captured data at a rate of 31.25 Hz over a duration of about 62 s. The sample size over this duration was 2048, yielding a frequency resolution of about 0.015 Hz, or 0.008 in terms of the Strouhal number. The actuation frequency was maintained within 1–2% of the targeted frequency. The uncertainty in the time- or ensemble-averaged velocity was 1.5% in air. The base pressure in air was measured with a capacitance-type differential pressure transducer (MKS Instruments), and the measurement uncertainty was less than 0.5% of the freestream dynamic pressure. Although the true value of the TR-PIV system used in water is in allowing the dynamics of the unsteady wake to be determined, the uncertainty in the mean was determined to be no greater than 10% of the local turbulence intensity (i.e., typical uncertainty of 4% of the freestream velocity).

A. Instantaneous Velocity Vectors

Representative plots of the velocity vectors for the experiment in water with the actuators on and off are shown in Fig. 5. Although the wake is very unsteady in time, coherent structures can be observed in the instantaneous images. With no actuation, the roll-up of the vortices in the shear layer is clearly present. A relatively large vortex can be seen on both sides of the centerline, but offset in the x direction. These counter-rotating vortices continue to roll up as they are convected downstream and maintain the offset between them. This behavior is consistent with the formation of a large-scale three-dimensional structure. In Fig. 5b, when the wake is subject to axisymmetric forcing at $St_e = 0.28$, a similar set of counter-rotating vortices on opposite sides of the centerline can be seen, although the vortices appear to be larger and much more coherent. The phase offset between the two structures is also much more apparent. Downstream of the recirculation region, the instantaneous velocity vectors indicate the presence of an asymmetric vortex structure that is likely related to the helical structure described in [13].

B. Mean Velocity

Ensemble averages of the instantaneous velocity vector fields are shown in Fig. 6. It is clear that the mean flow with and without excitation is axisymmetric, as also observed by Berger et al. [13]. In both cases, there are two regions of mean counter-rotating flow on either side of the wake centerline. Although the two mean flows appear quite similar, close inspection reveals that the size of the recirculation region has been reduced, with the actuators turned on for a symmetric excitation at $St_e = 0.28$. Although not shown, with a symmetric excitation at $St_e = 0.14$, no appreciable difference in the structure of the mean wake was observed.

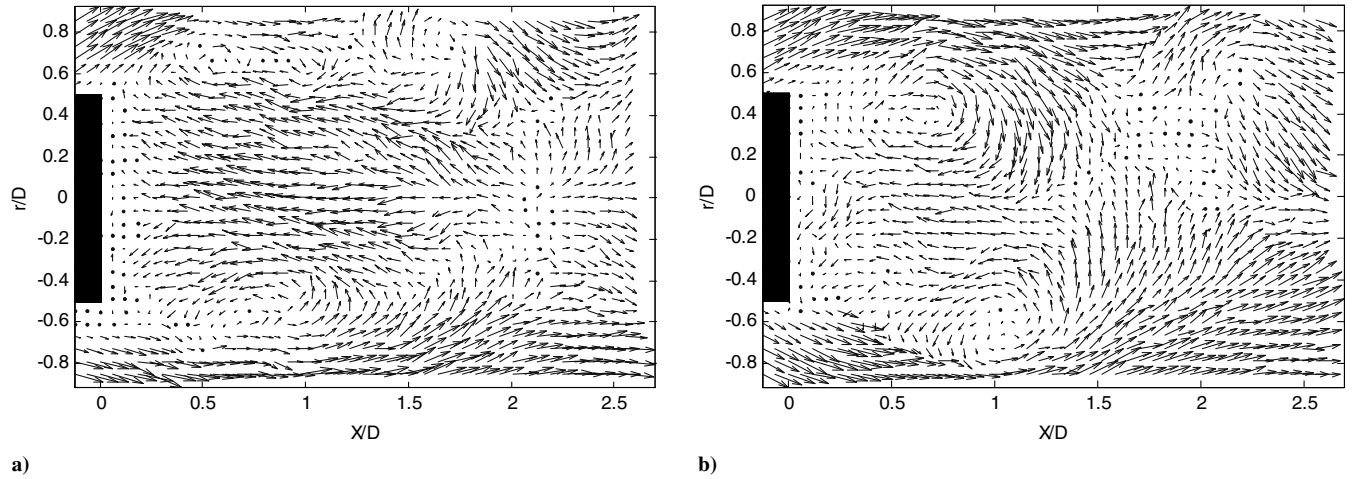

Fig. 5 Instantaneous velocity vector fields: a) no actuation and b) $St_e = 0.28$ symmetric actuation.

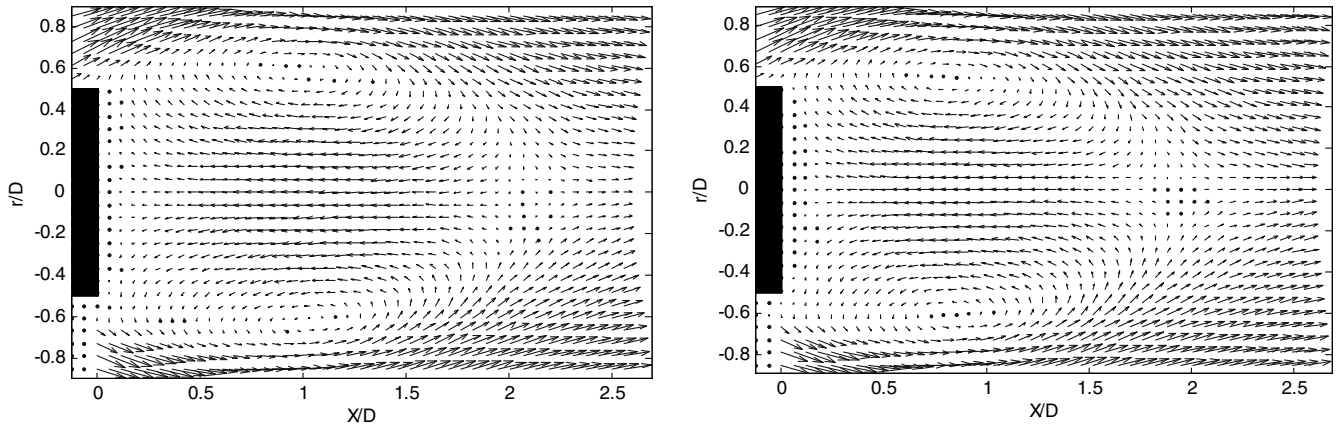

Fig. 6 Mean velocity vector fields: a) no actuation and b) $St_e = 0.28$ symmetric actuation.

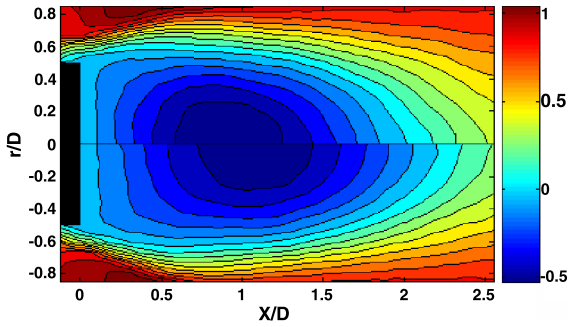

Fig. 7 Mean U/U_∞ contours for $St_e = 0.28$ symmetric actuation (top) with no actuation reference (bottom).

The effect of excitation on the mean flow is more evident in Fig. 7, in which contours of the mean streamwise velocity with and without excitation are shown. The contours for the excited and unexcited cases were split in half and placed together for a more direct comparison. It is clear that the axisymmetric forcing of the disk wake causes the mean wake to become shorter.

To compare the size of the recirculation region more directly, the zero-velocity contour lines were extracted and plotted on the same set of axes for the experiments in both air and water in Fig. 8. Symmetric actuation at twice the natural frequency ($St_e = 0.30$ for air and 0.28 for water) shows a comparable reduction in the size of the recirculation region in both air and water. The recirculation region is reduced both in length and width. In air, the addition of a helical excitation at the natural frequency caused a further reduction in size of the recirculation region. The reduction in the size of the wake recirculation region accompanied by the increased streamline curvature indicates that the base pressure is reduced with excitation. This was indeed confirmed by the base pressure measurement in the wind tunnel, as shown later. Thus, excitation has likely caused an increase in the mean drag of the disk.

Streamwise profiles of the mean velocity with and without excitation are shown at various positions in the wake in Fig. 9. Here, the left side shows the nonactuated wake and the right side shows the actuated wake. In the recirculation region at $x/D = 1$, the two profiles appear quite similar, with the magnitude of velocity in the recirculation region unchanged with excitation. Downstream at $x/D = 1.5$, the two profiles are different, due to the shortening of the recirculation region with actuation. Additionally, the nonactuated wake reaches zero velocity at $r/D = 0.5$, whereas the actuated wake crosses zero at about $r/D = 0.4$, showing the actuated wake to be narrower in the r direction than the nonactuated wake. Further downstream at $x/D = 2$ and 2.5, the actuated wake still has higher velocities near the centerline, showing that the trends continue beyond the end of the recirculation region. These results indicate that actuation causes the entire near wake to shift toward the trailing edge.

Streamwise velocity profiles taken along the centerline are presented in Fig. 10. In both air and water, the length of the nonactuated recirculation region is about $x/D = 2$, slightly shorter than the length of $x/D = 2.6$ found by Carmody [17], perhaps due to the hot-wire technique used in the reference. With the actuation turned on, the symmetric excitation mode causes a reduction in length of the recirculation region of 10% in both air and water. In air, the helical excitation caused a slightly larger reduction in the length of the recirculation region.

C. Velocity Fluctuations

The cross-stream turbulent velocity was extracted from the TR-PIV data and plotted as contours in Fig. 11. It is clear that the wake structure caused by the actuation has created greater lateral velocity fluctuations downstream of the recirculation region, with $St_e = 0.28$ symmetric actuation causing the highest fluctuations. This behavior is likely due to the promotion of the asymmetric wake structure shown in Fig. 5b.

Contours of the streamwise turbulent velocity profiles with and without excitation are shown in Fig. 12a. The highest fluctuation

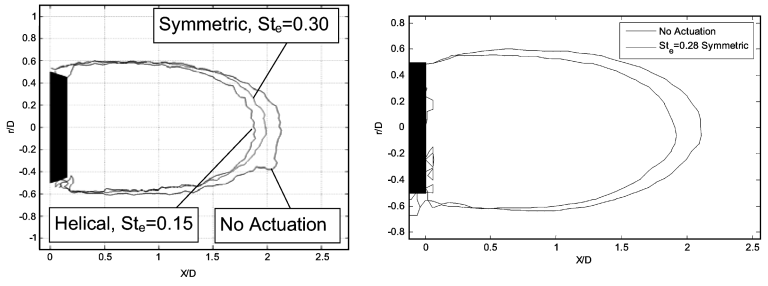

Fig. 8 Zero-velocity contours: a) wind-tunnel experiment and b) water-tunnel experiment.

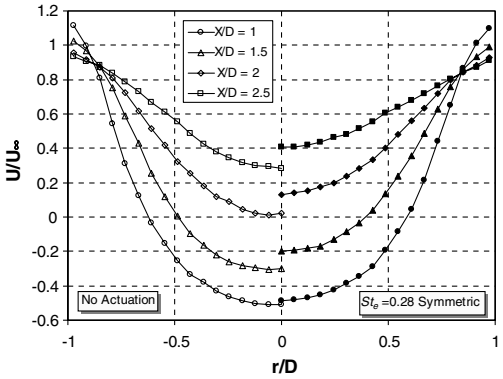

Fig. 9 Mean U-velocity profiles in water for no actuation (open symbols) and $St_e = 0.28$ symmetric actuation (filled symbols).

levels occur in the shear layer, as expected. Without excitation, the velocity fluctuations are the strongest in two regions: $x/D \sim 0.75$ and ~ 1.75. The first region may be due to high-frequency vortex pairing and the second region may be due to the presence of a larger vortex structure in the wake, such as those shown in Fig. 5. With excitation, the magnitude of the fluctuations in the shear layer increases downstream of $x/D \sim 0.5$; this causes a longer region of high rms turbulence intensity. Profiles from inside the shear layer to the centerline at $x/D = 1$ and 2.5 (Fig. 12b) confirm that velocity fluctuations are greater with the actuators on. The magnitude of the oscillations outside the shear layer, from $r/D = 0.75$ to about 1, are essentially identical with the actuators on and off, suggesting that the disturbances caused by the actuation take time to grow in the shear layers. Detailed investigation of the interaction between the actuation at the disk edge and the initial shear-layer development in the immediate wake is beyond the scope of the present experiment but warrants further study. Downstream at $x/D = 2.5$, the fluctuation levels are similar, because for both cases, this is beyond the recirculation region in which the asymmetric structure is dominant.

D. Frequency Analysis

The TR-PIV system has sufficient time resolution to allow spectra to be calculated at every point in the vector field. This allows for a variety of plotting options that enable regions of high energy to be quickly identified. One such method is to take power spectra for all r positions along a fixed x position and plot amplitude in contour form with the r direction on the y axis and frequency on the x axis. This resulted in symmetric plots on either side of the wake centerline, indicating the presence of significant velocity fluctuations in the shear layer. Results were essentially similar at a variety of streamwise positions. Here, $x/D = 2$ was chosen for comparison because the region of intense fluctuation in the shear layer is within the limits of the viewing window, as per Fig. 12a. This region was thought to most likely exhibit high-energy fluctuations in the frequency domain.

The nonactuated spectra were first compared with those with $St_e = 0.14$ symmetric actuation in Fig. 13a. The contours for no actuation show a peak at the natural frequency of $St = 0.14$, along with several other peaks at different frequencies. This suggests that there is energy in a variety of modes in the shear layer for the natural wake, as observed by Berger et al. [13]. With the actuation turned on, the peaks at frequencies in the shear layer other than the actuation frequency disappear, and all peaks vanish inside the recirculation bubble, indicating that the shear layer is quite receptive to forcing at this frequency. There is also a prominent low-frequency oscillation present across the entire disk wake, for which the significance is presently unclear but may be due to wake modulation caused by

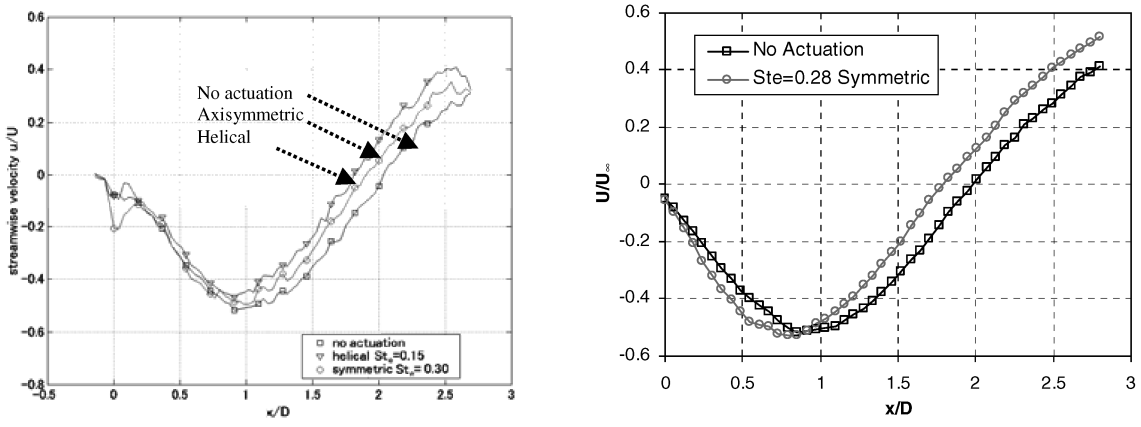

a) b)

Fig. 10 Streamwise velocity along centerline: a) wind-tunnel experiment and b) water-tunnel experiment.

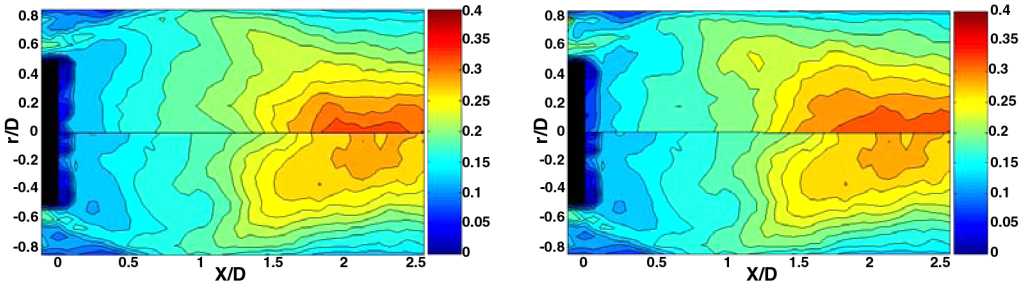

a) b)

Fig. 11 Radial turbulence distributions v'_{rms}/U_∞ with actuation on top and no actuation (reference) on bottom: a) $St_e = 0.14$ symmetric actuation and b) $St_e = 0.28$ symmetric actuation.

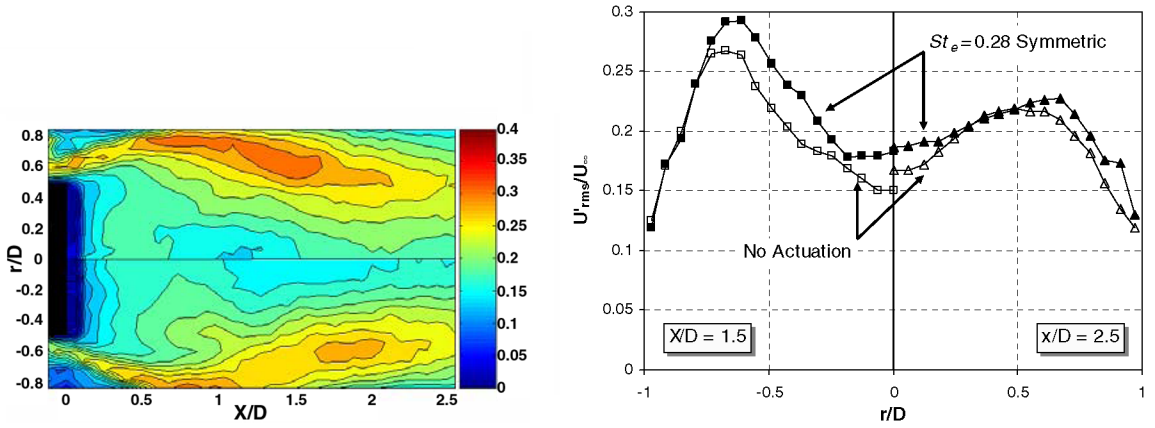

a) b)

Fig. 12 Axial turbulence distributions for $St_e = 0.28$ symmetric actuation: a) u'_{rms}/U_∞ contours with actuation on top and b) u'_{rms}/U_∞ profiles at $x/D = 1.5, 2.5$.

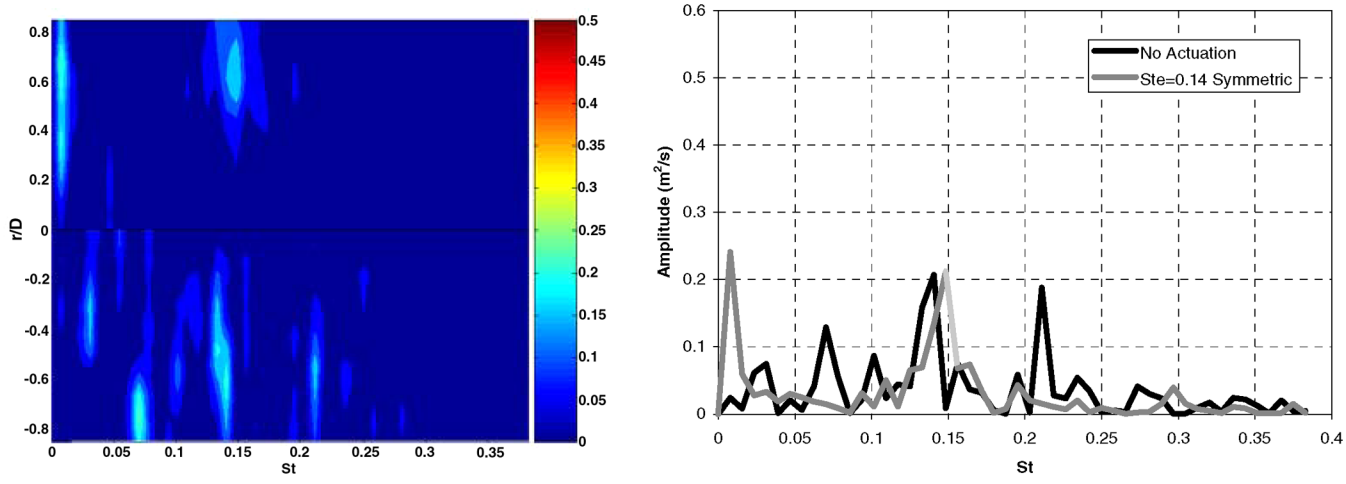

a) b)

Fig. 13 Power spectra for $St_e = 0.14$ symmetric actuation and no actuation: a) radial distribution of spectrum amplitude (m^2/s) at $x/D = 2$ with actuation on top and b) extracted power spectra at $x/D = 2$ and $r/D = 0.5$.

small differences in the forcing frequency and the instability of the wake, as discussed in the cylinder wake by Thiria and Wesfreid [18] and Mahir and Rockwell [19] (albeit at substantially lower Reynolds numbers). A sample power spectrum shown in Fig. 13b confirms that this low-frequency modulation is related to small differences in the forcing frequency and the natural frequency of the wake instability.

A similar comparison was performed for the case with $St_e = 0.28$ symmetric forcing. In this case, the contours (Fig. 14a) show a definite increase in energy, with actuation at the natural frequency of the shear-layer instability, $St_e = 0.14$, and remarkably, there is little evidence of the excitation frequency in the spectra. The extracted power spectrum (Fig. 14b) shows a peak at $St = 0.14$, with approximately 3 times the amplitude as the nonactuated peak, even though the amplitude of excitation is the same. This demonstrates clearly that under the axisymmetric excitation, the wake is much more receptive to forcing at twice the natural frequency as the natural frequency. In air, the axisymmetric excitation showed similar results in both the mean and fluctuating velocity fields; however, in this case, the wake was most receptive to helical actuation at the natural frequency (Fig. 10a).

Sample velocity-time traces used to produce these spectra are shown in Fig. 15. Visually, the traces appear to be anticorrelated, despite the symmetric actuation, and are consistent with the resulting excitation of the helical mode and observations from the instantaneous vectors of delayed vortex roll-up on opposite sides of the shear layer in the cross-sectional plane. Traces were also correlated on opposite sides of the centerline (i.e., trace at $r/D = -0.5$ correlated with $r/D = 0.5$, where the minus sign is used to denote the opposite direction), and the correlation coefficients between two traces were found to be negative. The amplitude was lowest for no actuation, increasing for $St_e = 0.14$ symmetric, and highest for $St_e = 0.28$, where the strongest anticorrelation occurred. This again shows that actuation is adding energy to the $St = 0.14$ mode in the shear layer.

E. Base Pressure in Air

The aforementioned reduction in size of the recirculation region corresponds to a decrease in base pressure (i.e., enhanced suction on the leeward surface of the disk). This can be observed in Fig. 16, in which the base pressure was measured in air at different actuation modes and frequencies. In addition to the axisymmetric and helical-mode excitations, a staggered excitation was tested in which three actuators are extended simultaneously and the three others remain flush with the disk, and vice versa. There is a phase difference of π between the two movements (refer to [16] for detail).

The base pressure is normalized by the base pressure for the no-actuation case. The figure shows the most prominent peak under the helical-mode excitation at a frequency matching the natural

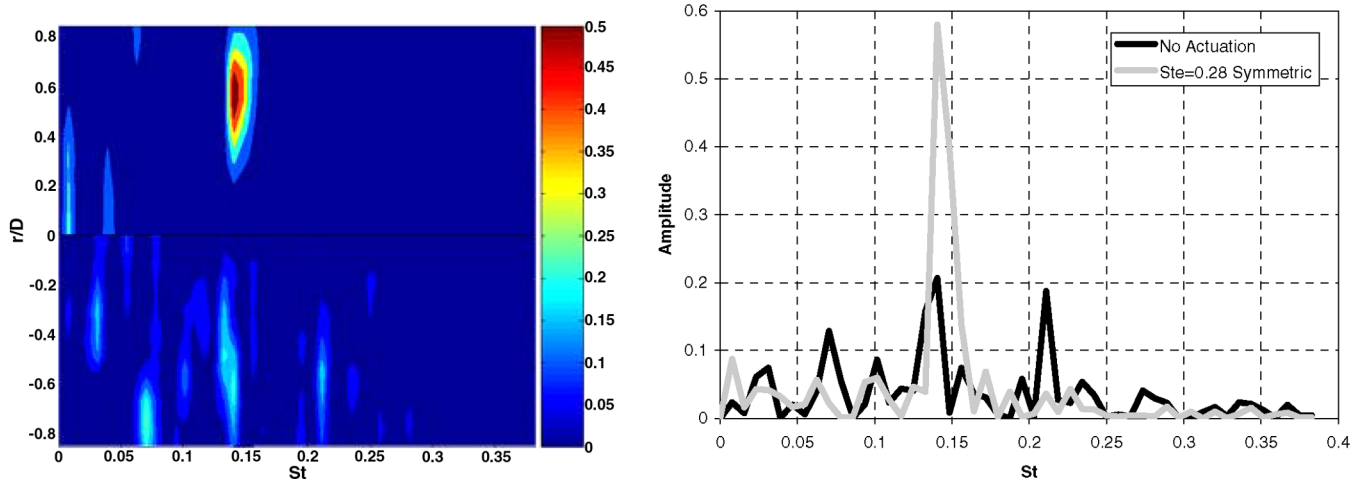

a) b)

Fig. 14 Power spectra for $St_e = 0.28$ symmetric actuation and no actuation: a) radial distribution of spectrum amplitude (m^2/s) at $x/D = 2$ with actuation on top and b) extracted power spectra at $x/D = 2$ and $r/D = 0.5$.

frequency. The rotational direction of the helical mode did not significantly affect the results. The axisymmetric-mode excitation is less effective, but shows a peak at double the frequency of the helical-mode natural frequency. Kim and Durbin [20], when exciting the shear layer around the recirculation region behind a sphere, also noted this same phenomenon. Their acoustic excitation was inherently symmetric and at the twice the frequency of the natural frequency. The staggered excitation did not produce a discernible effect, indicating that the shear-layer motion was not locked with the actuation, regardless of its frequency.

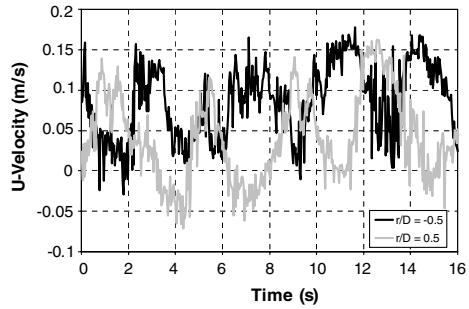

Fig. 15 Sample velocity-time series from TR-PIV at $X/D = 2$ for two radial locations on opposite sides of the centerline.

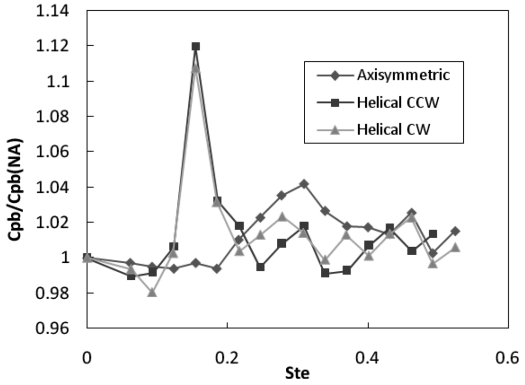

Fig. 16 Base pressure variation with actuations (actuation patterns: clockwise (CW), counterclockwise (CCW), downstream-facing direction).

IV. Further Discussion

Despite slight differences in geometry and natural frequency, the two wakes in air and water show remarkable similarity in recirculation-region length and in the turbulence profiles. It thus seems likely that in both cases that the actuator systems excited a similar large-scale vortex structure in the shear layer. Additionally, though the actuation signals were slightly different, forcing symmetrically at twice the natural-frequency-region size shrinks the length of the recirculation region about the same amount in air and water. This finding is similar to those of Chun and Sung [21], who forced the flow over a backward-facing step. In this case, they found that shear-layer forcing increased the turbulence and vorticity within the shear layer and thereby enhanced the entrainment. This resulted in a reduction in reattachment length, as found here. Though the flow configuration is different, it is likely that the same basic mechanism was at work for the reduction of the separation-bubble length by the shear-layer forcing.

A frequency analysis confirms that the wake is actually being forced into a helical mode at the subharmonic; similar behavior was also noted by Kim and Durbin [20]. Thus, it is expected that a further decrease in recirculation-region length could also be achieved in water by simply forcing the helical mode at the natural frequency as in air. Incidentally, as noted in [16], stationary tabs in an attempt to add longitudinal vortices in the wake did not produce any discernible effect on the wake unless tabs were extended to a fraction of the diameter.

The base pressure decrease (i.e., larger suction) corresponds to an increase in drag. Siegel [22] also found a similar increase in drag when actuating with a helical mode for a sting-mounted slender model. He recently extended his earlier experiment in water at a low Reynolds number to excite the double helical mode and establish planar symmetry in vortex-shedding [23]. Conversely, Jeon et al. [4] were able to decrease the drag behind a sphere by forcing relatively-high-frequency shear-layer instability waves themselves. Berger et al. [13] achieved a reduction in recirculation-region length with nutation, although drag was not measured. The reduction in the present study, however, was not as dramatic as the movement of the rear stagnation point to $x/D = 1.4$ noted by Berger et al. It seems that the excitation employed in [13] may have more effectively forced the helical mode than in the present investigation. In addition, Berger et al. found that the promotion of the helical mode caused a slight frequency change not found in the present study. To make definite conclusions, further study is required.

The current experiment has shown for the first time that the wake behind a disk can be controlled by similar means in both air and water. Although drag is increased, there are possible applications in

which increased drag and enhanced mixing under control are desirable, such as maneuverable aerodynamic decelerators [24] and disk-shaped flame holders. The wake has clearly responded to forcing, as indicated by the reduction in recirculation-region area. More important, when actuating at twice the natural frequency, the natural frequency itself is enhanced, showing that energy is added to the shear layer. The wake still remained axisymmetric in the mean, indicating that the dominant modes in the natural wake were still present. Additionally, the PIV systems proved to be an effective tool for investigating the flow: specifically, the TR-PIV that captured velocity-time traces at multiple points simultaneously without probes in the flow for the first time. Still, the ultimate goal remains to expand on the current results to gain full real-time active control. Henning and King [25] applied a closed-loop control to the flow over a backward-facing step, the flow somewhat analogous to the disk wake for its interplay among sharp-edge separation, base pressure, and extent of the recirculation zone. They fed back the surface pressure fluctuations near the reattachment region and controlled the spanwise reattachment length. The disk, however, poses a unique challenge with its three-dimensional multimode wake movement. It is thought that effective closed-loop feedback control of the disk wake can be implemented using a POD/mLSE algorithm, which has proven useful at suppressing separation over an airfoil at high angles of attack at Syracuse University [26]. Recently, an experiment [27] was performed on a blunt axisymmetric model on a magnetic suspension and balance system, and velocity field, base pressure, and forces and moments were measured, completely avoiding the support interference. The approach is also promising for the flow control behind axisymmetric bluff bodies.

V. Conclusions

The present experiment in both air and water to control the separated wake behind the disk with a fixed separation point has produced the following results. The open-loop actuations by the small-edge radial oscillation (in air) as well as small-momentum jets from the disk edge (in water) energized the shear-layer oscillation in helical or axisymmetric modes, depending on the frequency and phase of control actuation. The recirculation region was reduced most when the helical mode was enhanced, and different from delaying separation over curved-wall bluff bodies, the base pressure was also reduced. To suppress the vortical structure, a study on an active feedback control has been initiated.

Acknowledgments

This article was completed during H. Higuchi's recent stay at Tohoku University. Support from the Tohoku University Global Center of Excellence Program on World Center of Education and Research for Trans-Disciplinary Flow Dynamics is gratefully acknowledged. J. W. Hall would like to acknowledge funding from the Natural Sciences and Engineering Research Council of Canada. R. Bigger's original work was done as an undergraduate aerospace engineering student at Syracuse University under a NASA New York State Space Grant. The authors wish to acknowledge the following undergraduate students for their assistance during the earlier phase of the experiment: G. Gandlin, K. Sanada, and E. Turluer. Acknowledgment is also due to S. Ide's participation in the present project at Syracuse University. Discussion with J. Qiu, then at Tohoku University, on electromagnetic actuators was also crucial to start the experiment. Additional thanks go to D. Hunter, who built the actuator system for previous experiments, and to the machinists at both Tohoku University and Syracuse University, who built the models.

References

[1] Mehta, R. D., "Aerodynamics of Sports Balls," *Annual Review of Fluid Mechanics*, Vol. 17, 1985, pp. 151–189. doi:10.1146/annurev.fl.17.010185.001055

[2] Kiura, T., and Higuchi, H., "Knuckleball Aerodynamics: Passive Alteration of Three-Dimensional Wake-Structure Interactions," *IUTAM Symposium on Bluff Body Wakes and Vortex-Induced Vibrations*, Marseille, France, 13–16 June 2000.

[3] Higuchi, H., "Passive and Active Controls of Three-Dimensional Wake of Bluff Body," *JSME International Journal*, Vol. 48, No. 2, 2005, pp. 322–327.

[4] Jeon, S., Choi, J., Jeon, W., Choi, H., and Park, J., "Active Control over a Sphere for Drag Reduction at Subcritical Reynolds Number," *Journal of Fluid Mechanics*, Vol. 517, 2004, pp. 113–129. doi:10.1017/S0022112004000850

[5] Quass, B., Howard, F., Weinstein, L., and Bushnell, D., "Longitudinal Grooves for Bluff Body Drag Reduction," *AIAA Journal*, Vol. 19, No. 4, 1981, pp. 535–537. doi:10.2514/3.7793

[6] Amitay, M., Honohan, A. M., and Glezer, A., "Flow Control on a Two-Dimensional Circular Cylinder," *Third International Symposium on Turbulence and Shear Flow Phenomena*, Sendai, Japan, June 2003, pp. 561–566.

[7] Cannon, S. C., "Large-Scale Structures and the Spatial Evolution of Wakes Behind Axisymmetric Bluff Bodies," Ph.D. Dissertation, Univ. of Arizona, Tucson, AZ, 1991.

[8] Higuchi, H., Zhang, J., Furuya, S., and Muzas, B., "Immediate and Near Wake Flow Patterns Behind Slotted Disks," *AIAA Journal*, Vol. 36, No. 9, 1998, pp. 1626–1634. doi:10.2514/2.564

[9] Naudascher, E., "Flow in the Wake of Self-Propelled Bodies and Related Sources of Turbulence," *Journal of Fluid Mechanics*, Vol. 22, Pt. 4, 1965, pp. 625–656. doi:10.1017/S0022112065001039

[10] Higuchi, H., and Kubota, T., "Axisymmetric Wakes Behind a Slender Body Including the Zero-Momentum Configurations," *Physics of Fluids*, Vol. 2, No. 9, 1990, pp. 1615–1623. doi:10.1063/1.857569

[11] Willmarth, W. W., Hawk, N. E., and Harvey, R. L., "Steady and Unsteady Motions and Wakes of Freely Falling Disks," *Physics of Fluids*, Vol. 7, No. 2, Feb. 1964, pp. 197–208. doi:10.1063/1.1711133

[12] Higuchi, H., and Balligand, H., "Circulation Time-History and Onset of Three-Dimensional Vortex Shedding in the Wake Behind a Disk," *Proceedings of the Second International Symposium on Turbulence and Shear Flow Phenomena*, Vol. 1, 2001, pp. 301–306.

[13] Berger, E., Scholtz, D., and Schumm, M., "Coherent Vortex Structures in the Wake of a Sphere and Circular Disk at Rest and Under Forced Vibrations," *Journal of Fluids and Structures*, Vol. 4, No. 3, 1990, pp. 231–257. doi:10.1016/S0889-9746(05)80014-3

[14] Andino, M. Y., Braud, C., Glauser, M. N., Higuchi, H., and Van Langen, P., "Global Effects of Control Over a NACA 4412 Hydrofoil," 35th AIAA Fluid Dynamics Conference and Exhibit, Toronto, AIAA Paper 2005-4833, June 2005.

[15] Balligand, H., "Unsteady Wake Structure Behind a Solid Disk," Ph. D. Thesis, Syracuse Univ., Syracuse, NY, 2005.

[16] Higuchi, H., Ide, S., Qiu, J., and Tani, J., "Open-Loop Control of the Disk Wake with Electro-Magnetic Actuators," 2nd AIAA Flow Control Conference, Portland, OR, AIAA Paper 2004-2321, 2004.

[17] Carmody, T., "Establishment of the Wake Behind a Disk," *Journal of Basic Engineering*, Dec. 1964, pp. 869–882.

[18] Thiria, B., and Wesfreid, J. E., "Stability Properties of Forced Wakes," *Journal of Fluid Mechanics*, Vol. 579, 2007, pp. 137–161. doi:10.1017/S0022112007004818

[19] Mahir, N., and Rockwell, D., "Vortex Formation from a Forced System of Two Cylinders, Part 1: Tandem Arrangement," *Journal of Fluids and Structures*, Vol. 10, No. 5, 1996, pp. 473–489. doi:10.1006/jfls.1996.0032

[20] Kim, D., and Durbin, P. A., "Observations of the Frequencies in a Sphere Wake and Drag Increase by Acoustic Excitations," *Physics of Fluids*, Vol. 31, 1988, pp. 3260–3265. doi:10.1063/1.866937

[21] Chun, K. B., and Sung, H. J., "Control of Turbulent Separated Flow over a Backward-Facing Step by Local Forcing," *Experiments in Fluids*, Vol. 21, No. 6, 1996, pp. 417–426.

[22] Siegel, S., "Experimental Investigation of the Wake Behind an Axisymmetric Bluff Body," Ph.D. Dissertation, Univ. of Arizona, Tucson, AZ, 1999.

[23] Siegel, S., Seidel, J., Cohen, K., Aradag, S., and McLaughlin, T., "Open Loop Transient Forcing of an Axisymmetric Bluff Body Wake," AIAA Paper 2008-595, 2008.

[24] Teramoto, S., Hiraki, K., and Fujii, K., "Numerical Analysis of Dynamic Stability of a Reentry Capsule at Transonic Speeds," *AIAA*

Journal, Vol. 39, No. 4, 2001, pp. 646–653.
doi:10.2514/2.1357
[25] Henning, L., and King, R., "Robust Multivariable Closed-Loop Control of a Turbulent Backward-Facing Step Flow, " *Journal of Aircraft*, Vol. 44, No. 1, 2007, pp. 201–208.
doi:10.2514/1.22934
[26] Pinier, J. T., Ausseur, J., Glauser, M. N., and Higuchi, H., "Proportional Closed-Loop Feedback Control Of Flow Separation," *AIAA Journal*, Vol. 45, No. 1, 2007, pp. 181–190.
doi:10.2514/1.23465
[27] Higuchi, H., Sawada, H., and Kato, H., "Sting-Free Measurements on a Magnetically Supported Right Circular Cylinder Aligned with the Free Stream," *Journal of Fluid Mechanics*, Vol. 596, 2008, pp. 49–72.
doi:10.1017/S0022112007008956

F. Coton
Associate Editor